Vibration frequency analysis of rippled single-layered graphene sheet: Toward the nano resonant devices design

Zeyi Zhang[a,b], Lan Lan[c], Yafei Wang[a,b], Changguo Wang[a,b,*]

[a] Center for Composite Materials and Structures, Harbin Institute of Technology, Harbin, 150001, PR China
[b] National Key Laboratory of Science and Technology for National Defence on Advanced Composites in Special Environments, Harbin Institute of Technology, Harbin, 150080, PR China
[c] Shanghai YS Information Technology Co., Ltd., Shanghai, 200240, PR China

ARTICLE INFO

ABSTRACT

This paper studies the vibration frequency of rippled single-layered graphene sheets (SLGSs). The energy-based analytical model is proposed based on improved continuum mechanics theory (CMT) by considering the variable vibration mass and strain energy. It is found that significant frequency shift on pristine SLGSs can be realized using functional groups, defects, carbon nanotubes and surface wrinkles. Reduction of vibration frequency in SLGSs with random ripples is mainly dominated by the variable mass. Increasing of vibration frequency in continuously rippled SLGSs is highly warranted by the strain energy. A phase diagram which shows the relationship between different factors causing ripples on SLGS and frequency shift can be obtained. Finally, a novel nano device concept can be proposed based on frequency ascension, quality factors and bandwidth. The results obtained in this paper can provide a fundamental understanding of tunable vibration frequency in atomically thin materials and an insight for the next generation nano resonant devices design.

1. Introduction

Since the discovery of mechanically exfoliated graphene [1,2], the single-layered graphene sheet (SLGS) has received immense attention of the scientific community due to its exceptional physical properties [3–5]. The high vibration frequency and high sensitivity give them the ability to be used in various graphene-based nano resonant devices. Thus, understanding the vibration behavior of SLGS is an essential task for designing graphene-based nanomechanical resonator [6], mass detection devices [7], and nanoelectromechanical systems (NEMS) featuring resonant frequencies close to the terahertz range [8]. These properties of SLGSs have long warranted a number of applications in various domains of science and technology [9–11].

Pioneering experiments [12,13] demonstrated that random ripples spontaneously appear on the single layer of graphene owing to its two-dimensional (2D) intrinsic attribute and topological defects. Moreover, chemically vapor deposition (CVD) [14–17] method is applied to produce graphene for industrial scale. Certain functional groups or defects inevitably occur on the surface of graphene sheets during the course of production. Meyer et al. [18] investigated ripples in suspended graphene through experimental observation. He et al. [19] reported a molecular dynamics (MD) simulation of ripple propagation in graphene. Iyakutti et al. [20] simulated and analyzed the formation of ripples in SLGSs in both membrane and ribbon conformations. Researchers revealed that the natural vibration frequency of SLGS is closely sensitive to its configurations, which is related to mass [7] and strain [21].

For analysis of graphene, common practices to investigate the vibration are based on continuum mechanics theory (CMT) which has been validated by molecular dynamics (MD) simulation [22–25]. Inui et al. [26] introduced CMT to study the equilibrium shape of SLGS suspended over a silicon substrate with a narrow gap and unveiled the vibration frequency response in a SLGS by collision with an argon cluster. Atalaya et al. [27] established a more simplified theoretical framework with respect to CMT for modeling the vibration properties of suspended graphene sheets. They found the nonlinearity process of proposed theory is necessary and deflection threshold is on the order of 0.5 Å. Zhang et al. [28] investigated the free vibration behavior of SLGS using a continuum model, which combined the Eringen nonlocal constitutive equation with the classical plate theory. Additionally, many carbon-based nanostructures can be considered as deformed graphene sheets. Employing classical method (such as CMT) is also useful to analyze the vibration frequency of multi-layered graphene sheets (MLGS) [29] and carbon nanotubes (CNT) [30].

---

* Corresponding author. Center for Composite Materials and Structures, Harbin Institute of Technology, Harbin, 150001, PR China.
  E-mail address: wangcg@hit.edu.cn (C. Wang).

Unfortunately, to our best of knowledge, it appears that there has been only limit research into the vibration frequency of rippled SLGSs using CMT, and it is especially true that little work has been done on the problem of variable mass effect and energy-based model. In order to guide the design of nano resonant devices in the next generation, it is essential to develop efficient closed-form expressions for the vibration frequency of rippled SLGSs without the need of conducting expensive and time-consuming MD simulations or laboratory experiments.

In this work, we study the influence of the variable mass involved in vibration and strain energy on the vibration frequency of rippled SLGSs. The structure of this paper is organized as follows. **Section 2** describes the theory model and specific methods of the improved continuum mechanics theory (CMT) for graphene sheets. **Section 3** is devoted to the discussion of the influence on the SLGSs vibration frequency induced by different kinds of ripples, taking functional groups, defects, wrinkles and van der Waals interaction-driven ripples as examples. Moreover, the influence of the distribution manner of ripples on the graphene sheets is also discussed in this section. **Section 4** ends with a summary of the crucial conclusions.

2. Computational method and theoretical model

2.1. Improved continuum mechanics theory

Based on continuum mechanics theory (CMT) and energy method, the vibration frequency of single-layered graphene sheets (SLGSs) can be obtained by

$$T_{\max} = U_{\max} \tag{1}$$

The variable mass and strain energy incurred by ripples have great influences on the vibration characteristics of SLGSs. Here, the variable mass involved in vibration, $\Delta\rho_S$, dominates the maximum kinetic energy of the system $T_{\max}$, and the strain energy contributes to the maximum potential energy of the system $U_{\max}$.

The maximum kinetic energy $T_{\max}$ of rippled SLGS is

$$T_{\max} = T_{\max}^0 + \Delta T = T_{\max}^0 + \frac{1}{2}(2\pi f)^2 \int_{A'} \Delta\rho_S W^2(x, y) dA' \tag{2}$$

where $T_{\max}^0$ is the maximum kinetic energy of pristine graphene, f is the vibration frequency of rippled SLGSs, A' is the area of the deformed region. W is the vibration mode function. $\Delta\rho_S$ is the variable mass induced by ripples. For instance, the calculation method of $\Delta\rho_S$ of functionalized rippled SLGS can be seen in Fig. 1 (a).

Here the graphene is considered as an isotropous thin plate. Assuming that the graphene analysis model contains n_C carbon atoms, the spatial area occupied by the model before the configuration changes is S, the total mass is M_c, the surface density $\rho_s = M_c/S$. After the configuration changes, the space area that the carbon atoms occupy is s, the total mass is $M_c + \Delta M + M_r$, in which ΔM is the change of carbon mass in this rippled region, M_r is the mass of the increased or decreased

atomics such as functional groups or defects. Then the surface density changes into $\rho_s = (M_c + \Delta M + M_r)/s$. Total variable mass involved in vibration resulting from ripple $\Delta\rho_S$ is expressed as the sum of $\Delta\rho_S^{mass}$ and $\Delta\rho_S^{geom}$, in which $\Delta\rho_S^{mass}$ refers to the atomic mass increase or decrease in the local area due to ripples. $\Delta\rho_S^{geom}$ indicates the effective vibration variable mass per unit area due to the changes of the local projection area. Expression for $\Delta\rho_S$ is derived as

$$\Delta\rho_S = \Delta\rho_S^{mass} + \Delta\rho_S^{geom} = \frac{\Delta M + M_r}{s} + \left(\frac{M_c}{s} - \frac{M_c}{S}\right)$$
$$= \frac{\Delta M + M_r}{s} + \rho_S(S/s - 1) \tag{3}$$

The maximum potential energy $U_{\max}$ of the rippled SLGSs can be expressed as

$$U_{\max}(\varepsilon_{0x}, \varepsilon_{0y}) = U_{\max}^0 + \Delta U = U_{\max}^0$$
$$+ \frac{1}{2}\iint_{A'} \frac{Eh}{1-\mu^2}(\varepsilon_{0x}^2 + \varepsilon_{0y}^2 + 2\mu\varepsilon_{0x}\varepsilon_{0y})dxdy \tag{4}$$

where is the maximum potential energy of pristine graphene. The initial prestrain ε_0 is the key parameter of the maximum potential energy of the system $U_{\max}$. The calculation model of the initial prestrain in x, y direction ε_{0x}, ε_{0y} is established in Fig. 1 (b).

$$\varepsilon_{0x} = \frac{l_2' - l_2}{l_2}, \ \varepsilon_{0y} = \frac{l_1' - l_1}{l_1} \tag{5}$$

Based on Equations (1)–(5), when the damping effect is ignored, the vibration frequency of rippled SLGSs is derived as

$$f = \frac{1}{2\pi}\sqrt{\frac{2U_{\max}(\varepsilon_{0x}, \varepsilon_{0y})}{\int_A \rho_S W^2(x, y)dA + \int_{A'} \Delta\rho_S W^2(x, y)dA'}} \tag{6}$$

The vibration frequency variation of functionalized graphene or SLGS with defects is induced by the increase or decrease of local vibration mass. In other case, when wrinkles exist on SLGS due to external mechanical loading, the vibration frequency of wrinkled SLGS shifts on account of configuration change. Based on Equation (3), $\Delta\rho_S$ of wrinkled SLGS is only consist of $\Delta\rho_S^{geom}$, which can be expressed as

$$\Delta\rho_s^w = \frac{M_c}{s} - \frac{M_c}{S} = \rho_S\left(\frac{S}{s} - 1\right) \tag{7}$$

Taking the rectangular graphene shear wrinkle analysis model as an example, the strain energy per unit area Δu_g can be obtained based on the research of Wong [31].

$$\Delta u_g(\gamma_g) = \frac{E_g h_g^3}{24(1-\mu_g^2)}\frac{\pi^4 A_g^2}{4\lambda_{g-1}^4} + \frac{E_g h_g}{2}\frac{\gamma_g^2}{4} + \frac{E_g h_g}{2}\frac{\pi^2 A_g^2 \gamma_g}{8\lambda_{g-2}^2} \tag{8}$$

where γ_g is shear strain of rectangular SLGS, A_g is average wrinkle amplitude of graphene, λ_{g-1} is the average half wavelength along the direction of the wrinkle texture, λ_{g-2} is the average half wavelength along the direction of the wrinkles of graphene.

Based on Equation (6), the vibration frequency of wrinkled rectangular graphene can be expressed as

$$f^w = \frac{1}{2\pi}\sqrt{\frac{\{\frac{\pi^4}{a^4}\{D_{g-11}A_x^4 + D_{g-11}A_y^4\frac{a^4}{b^4} + \frac{2a^2}{b^2}[D_{g-12}B_xB_y + 2D_{g-66}C_xC_y]\} + \frac{\Delta u_g(\gamma_g)}{F_{x-2}\cdot F_{y-2}}\}}{\rho_S + \Delta\rho_S}} \tag{9}$$

where F_{x-2}, F_{y-2} are the determining factors of vibration frequency. D_{g-ij} is the component of the bending stiffness matrix. A_x, A_y, B_x, B_y, C_x, C_y are integration constants which are related to boundary conditions and the concrete vibration modal orders.

2.2. The influence of distribution manner on vibration frequency

According to the Equation (6) and Fig. 2, the vibration frequency f^C of the continuously functionalized rippled SLGSs or graphene with
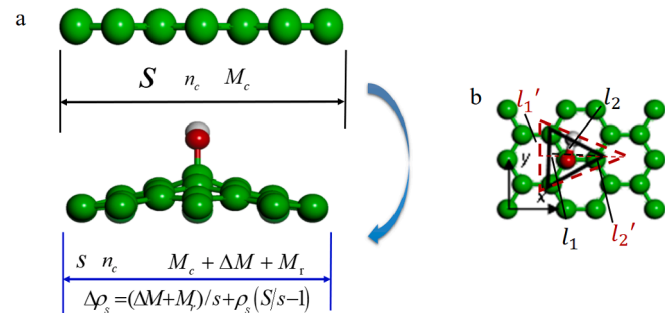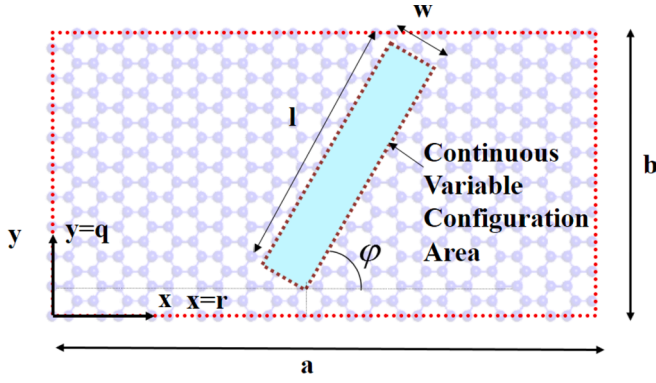

Fig. 1. (a) The variable mass model of rippled SLGS. (b) The prestrain calculation model of rippled SLGS. (A colour version of this figure can be viewed online.)

Fig. 2. Graphene analysis model with continuous functional groups. The length-fineness ratio: a/b. (A colour version of this figure can be viewed online.)

defects is

$$f^C = \frac{1}{2\pi}\sqrt{\frac{\{\frac{\pi^4}{a^4}[D_{g-11}A_x^4 + D_{g-11}A_y^4 \frac{a^4}{b^4} + \frac{2a^2}{b^2}[D_{g-12}B_xB_y + 2D_{g-66}C_xC_y]] + \frac{\Delta u_g}{F_{x-2}\cdot F_{y-2}}\}}{\rho_S + \Delta\rho_S^C\cdot F_{x-\text{int}}|_r^{r+w\sin\phi+l\cos\phi}\cdot F_{y-\text{int}}|_q^{q+w\cos\phi+l\sin\phi}/(F_{x-2}\cdot F_{y-2})}}$$
(10)

where $F_{x-\text{int}}$, $F_{y-\text{int}}$ are the determining factors of vibration frequency. (r, q) is the spatial coordinates of the bottom point in the continuous rippled region. w and l are width and length of the continuous rippled region, respectively. ϕ is the angle between the rippled region and x-direction.

The strain energy per unit area can be expressed as

$$\Delta u_g = \frac{Eh}{2(1 - \mu^2)}(\varepsilon_{0x}^2 + \varepsilon_{0y}^2 + 2\mu\varepsilon_{0x}\varepsilon_{0y})$$
(11)

For the randomly functionalized SLGSs, the effect of Δu_g on the vibration frequency is negligible,

$$f^R = \frac{\pi}{2a^2}\sqrt{\frac{D_{g-11}A_x^4 + D_{g-11}A_y^4\frac{a^4}{b^4} + \frac{2a^2}{b^2}[D_{g-12}B_xB_y + 2D_{g-66}C_xC_y]}{\rho_S + \Delta m\sum_{i=1}^{n_R} W^2(x_i, y_i)/(F_{x-2}\cdot F_{y-2})}}$$
(12)

where Δm is the variable vibration mass, n_R is the number of random functional groups, (x_i, y_i) is the coordinate of functional groups.

In particular, when $\Delta T = 0$, $\Delta U = 0$, $T_{\max}^0 = U_{\max}^0$, Equation (12) can be simplified to Equation (10), i.e., the vibration frequency of pristine graphene.

$$f^0 = \frac{\pi}{2a^2\sqrt{\rho_S}}\sqrt{D_{g-11}A_x^4 + D_{g-11}A_y^4\frac{a^4}{b^4} + \frac{2a^2}{b^2}[D_{g-12}B_xB_y + 2D_{g-66}C_xC_y]}$$
(13)

Compared with the classical CMT, our method fully considers the effect of local vibration mass change and strain energy on the vibration frequency of rippled SLGS. Here we define our method as improved CMT.

3. Results and discussion

3.1. Validation for the vibration frequency prediction model

Results are presented for the vibration frequencies based on the equations proposed in the preceding section and validated with the experimental results in the reference [8,32], as shown in Fig. 3. The error range can be controlled within 1.29% and the numerical values of vibration frequencies for different sizes and conditions are found to be in excellent agreement with those reported in literature. In addition, as illustrated in Fig. 4, the vibrational modes of the SLGSs in Ref. [32] are analyzed by our method, and the results are compared with the experimental and FEM results in Ref. [32]. It is observed that the results
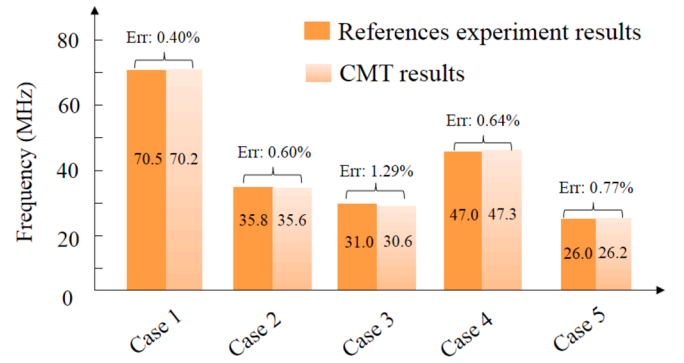

Fig. 3. Comparisons of our simulation results with experimental results in Refs. [8,32]. The thickness of SLGSs of case 1–5 are considered as 0.3 nm, 5 nm, 11 nm, 5 nm and 10 nm, respectively. (A colour version of this figure can be viewed online.)

that our improved CMT are accurate which can be used to predict the vibration frequency of SLGSs.

To verify the reliability of our method in predicting the vibration frequency of rippled SLGS, a comparison between the results of MD simulation and prediction results based on our method is performed under the same boundary and loading conditions. In molecular dynamics (MD) simulations, the interactions are modeled using the Compass Force Field and the boundary carbon atoms on the left and right edges of the SLGSs are fixed. We first carried out geometry optimizations and chose ultra-fine as the appointed calculation quality. Meanwhile the maximum iteration was 5000. Next dynamic simulations were performed on the optimized models in the NVE (the constant-number of particles, constant-volume, and constant-energy) ensemble. In the simulations, the NVE ensemble guaranteed total energy conservation [33]. The time step was 1 fs. The total simulation times were 20ps-100ps (determined by the different sizes of the model). The initial temperature of the simulation systems was around 300 K. In addition, the kinetic energy and potential energy can be transformed into each other in the simulation system. That is to say, the vibration frequencies can be computed using the fast Fourier transform method corresponding to the transformation process. Taking wrinkled SLGS as an example, the vibration frequency of wrinkled SLGS vs. shear strain are presented in Fig. 5. The average relative deviation between the results of wrinkled SLGS based on our improved continuum mechanics theory and MD simulation results is about 3.4% which fit well.
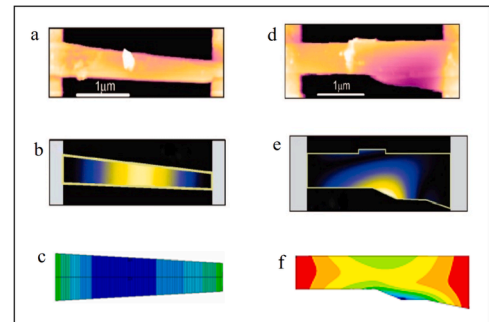

Fig. 4. Comparisons among our results, experiments and simulations in Ref. [32]. (a–c) Experiment measured topography, shape of the eigenmode at 31 MHz obtained using FEM simulations and our simulation results of SLGS with no buckling, respectively. t = 11 nm, l = 2.8 μm, $w_{\min} = 0.3$ μm, and $w_{\max} = 0.5$ μm. (d–f) Experiment measured topography, shape of the first eigenmode obtained using FEM simulations and our simulation results of SLGS with local buckling, respectively. t = 6 nm, l = 2.8 μm, $w_{\min} = 0.5$ μm, and $w_{\max} = 0.8$ μm. The maximum out-of-plane displacement of the buckling is 37 nm. (A colour version of this figure can be viewed online.)
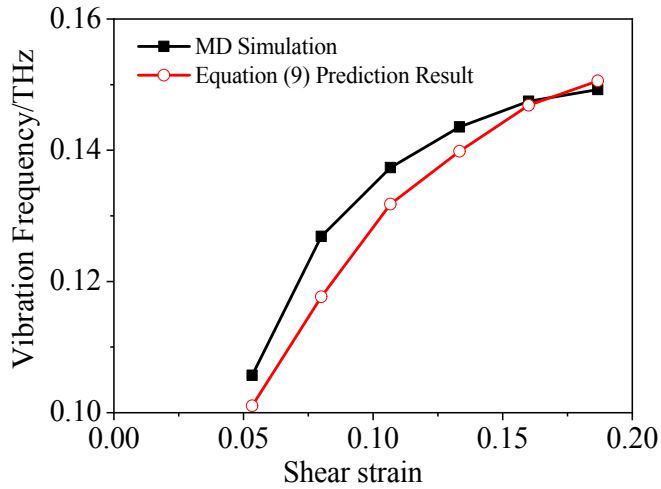
Fig. 5. Comparison of vibration frequencies for wrinkled graphene between simulation and prediction. (A colour version of this figure can be viewed online).

3.2. Rippled SLGS due to variable vibration mass

We have presented computationally efficient analytical closed-form expressions for the vibration frequency of rippled SLGSs, wherein the ripples may be induced by functional groups or defects. It is important to note that the distribution manners of ripples have different influences on the vibration frequency shift. A single functional group or defect can induce a local ripple, as illustrated in Table 1. It is noteworthy that continuous distribution of functional groups can induce global Gaussian curvature bending configuration on SLGS.

When –OH functional groups continuously distribute on SLGS, the local variable vibration mass per unit area $\Delta\rho_{SC}^{-OH}$ is 0.56×10^{-6} kg/m². The prestrain in x-direction and y-direction induced by continuous –OH functional groups, ε_{0x}^{-OH} and ε_{0y}^{-OH}, are 0.16 and 0.25, respectively. The case of a SLGS with random distribution of functional groups can be reduced to a SLGS with a single ripple (i.e. a single –OH functional group). Similarly, the local variable vibration mass per unit area $\Delta\rho_{SR}^{-OH}$ is 1.04×10^{-6} kg/m². ε_{0x}^{-OH} is 0.017, ε_{0y}^{-OH} is 0.002. The surface density of pristine graphene is about 0.74×10^{-6} kg/m² [34], which is in similar order of magnitude with $\Delta\rho_{SR}^{-OH}$ and $\Delta\rho_{SC}^{-OH}$. From this perspective, the local variable vibration mass induced by functional groups will affect the vibration frequency of graphene inevitably. Nevertheless, the prestrain energy of a single –OH functional group is only 10^{-2} times as that brought by the continuous distribution of –OH functional groups. Hence, for rippled SLGS induced by continuously distributed functional groups, the variations in stiffness and mass are equally important to the frequency of the SLGSs. In the case of randomly distributed functional groups on SLGSs, it can be discerned that the change of vibration

Table 1
Local configuration change caused by continuous or random distribution of functional groups.
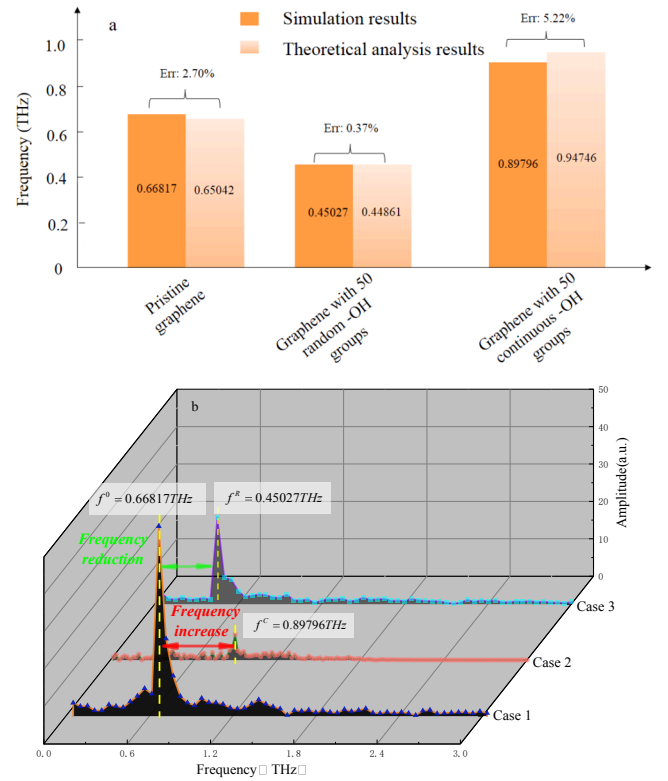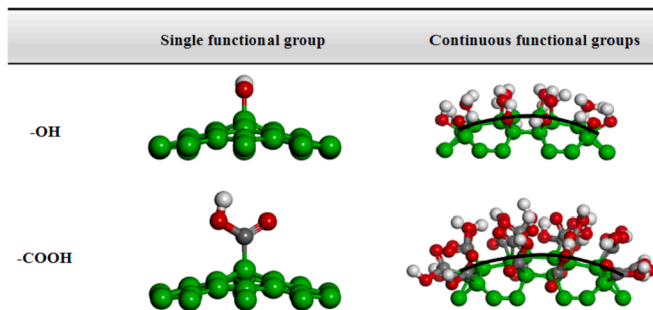

Fig. 6. (a) Comparisons between equation results and MD simulation results. (b) The vibration frequency and its shifts of the SLGS with different distribution manners of functional groups. Case 1–3 are pristine SLGS, SLGS with 50 continuously distributed –OH and SLGS with 50 randomly distributed –OH, respectively. (A colour version of this figure can be viewed online.)
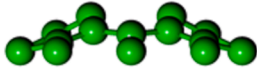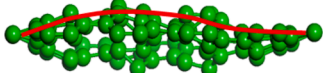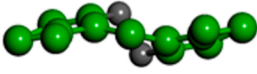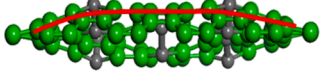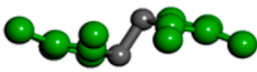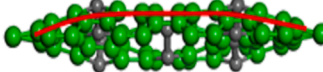
frequency actually depends on the local vibration mass change rather than the prestrain energy. The calculation results are given in Appendix A in detail.

Considering a 0.34 nm thick SLGS with 50 –OH groups, based on the Equations (10), (12) and (13), the vibration frequencies are shown in Fig. 6 (a). The frequency variation range Δf is about 0.2–0.3 THz, and the functional groups induce 69%–146% frequency shift on pristine SLGSs (from our method). Fig. 6 (b) reveals that the possible frequency shift ranges from 0.45027 THz to 0.89796 THz with variable distribution manners of the functional groups.

For SLGS with continuously or randomly distributed defects (Table 2), the calculation method is basically the same. However, the selected analysis cells are different. The relevant calculation results are given in Appendix B. When functional groups or defects continuously distributed on the SLGS, with the increase of the size *l* of the continuous deformation region the influence of local vibration mass on the kinetic energy of the system enhances. In addition to the vacancy defect, when the continuous deformation region expands, the initial prestrain energy will exert a reduced effect on the increase of free vibration frequency of SLGS, as shown in Fig. 7 (a). For –COOH functional groups with continuous distribution, the frequency shift can reach 0.33 THz at most, and the frequency tunable range is about 0.08 THz. In Fig. 7 (b), the frequency shift of rippled SLGS with continuously distributed –COOH functional groups can reach the maximum of 0.4 THz at 0°, and the frequency tunable range expands to 0.16 THz.

The relationship between the vibration frequency of rippled SLGS and the defects and functional groups number can be indicated in Fig.7 (c) based on Equation (12). The amplitude of variation of vibration frequency is positively correlated with the distribution ratio of functional groups or defects. In the case of randomly distributed functional groups or defects on SLGSs, as the effect induced by prestrain energy is

Table 2
Local configuration change caused by continuous or random distribution of defects.

in a small order of magnitude and can be ignored, the change of vibration frequency actually depends on the local vibration mass change rather than the prestrain energy. Therefore, -COOH, -OH functional groups, 5775-defects and 585-defects have the effects of reducing vibration frequency, in contrast, vacancy defects promote increasing vibration frequency. With the increase of the distribution proportion of random multipoint defects or functional groups, the influence caused by the change of vibration mass will be magnified. In other words, through increasing the numbers of functional groups or defects attached on SLSGs, the vibration frequency change will be more obvious.

Based on Equation (12), the frequency shift of multipoint randomly distributed rippled SLGSs is analyzed. The vibration frequency of
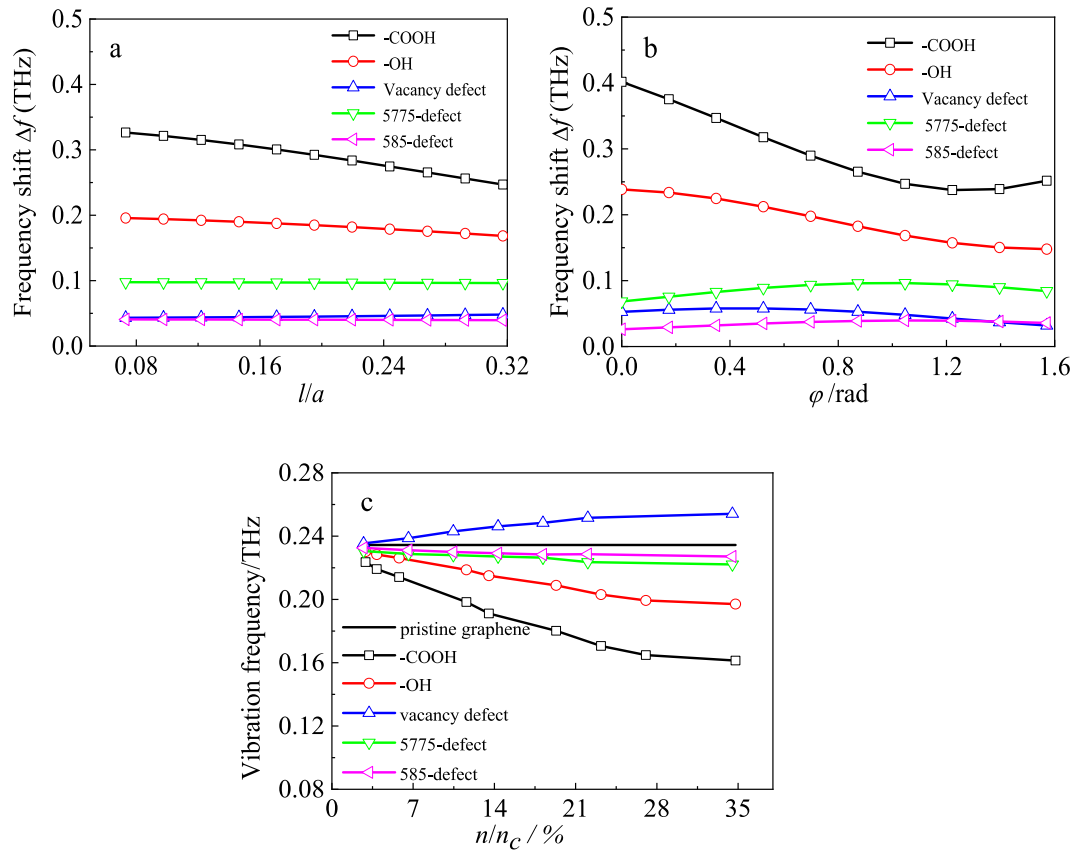

Fig. 7. Relationships between (a) dimensionless continuous variable configuration geometric size and frequency shift. $\varphi = \pi/3$, q = 0.62 nm , r = 2.27 nm , w = 0.21 nm , l = 0.43–1.85 nm. (b) continuous variable configuration distribution angle and frequency shift. q = 0.62 nm , r = 2.27 nm , l = 1.85 nm, w = 0.21 nm , $\varphi = 0 - \pi/2$. (c) distribution ratio of multiple random ripples and vibration frequencies of SLGS. (A colour version of this figure can be viewed online.)

rippled SLGS is positively correlated with the ratio of functional groups or defects. The increment of local vibration mass induced by the functional groups or the defects has the following relation, $\Delta m_{-COOH} > \Delta m_{-OH} > \Delta m_{5775-def} > \Delta m_{585-def} > 0 > \Delta m_{vac-def}$ (the corresponding values are 7.44×10^{-26} kg, 2.79×10^{-26} kg, 1.46×10^{-26} kg, 1.12×10^{-26} kg and -3.41×10^{-26} kg, respectively). When we put these five functional groups or defects on SLGS randomly, with the ratio $n_R/n_c = 35\%$, the frequency shift can reach 68.9%–108.4%. Therefore, functional groups (-COOH and –OH) and defects (5775-defects and 585-defects) contribute to frequency reduction, and frequency increment can be realized by vacancy defects. From the perspective of frequency control, reasonably distributed functional groups or defect on the rippled graphene surface makes it possible to efficiently tune the free vibration frequency of SLGS. When it comes to rippled SLGS with single functional group or defect, i.e. $n_R = 1$, according to the Saint-Venant principle, the single ripple has little influence on the free vibration frequency of graphene. With the increase of the length-fineness ratio (see Fig. 2) the relative deviation between the vibration frequency of single point deformation configuration graphene and that of pristine graphene gradually decreases.

3.3. Load-driven and van der waals interaction-driven rippled SLGS

Different from SLGS configuration change controlled by various vibration mass, rippled SLGS with wrinkles caused by applied mechanical load [35–37] has a much wider frequency shift range. Based on Equation (9), when the applied shear strain is less than 0.2, off-plane motion and in-plane translation occur of among carbon-carbon atoms, and the local vibration mass change caused by wrinkles can be ignored, i.e., the vibration frequency shift is mainly controlled by strain energy. The applied shear strain 0.2 leads to a nearly 150% increase in rippled SLGS vibration frequency. The vibration modes of the rippled SLGS are similar to the wrinkles waveform, as illustrated in Fig. 8 (a) and (b), thus the vibration of rippled SLGS is actually the vibration of the wrinkle region. When ripples appear on the SLGS driven only by van der Waals interaction, for instance, an Armchair CNT is placed above SLGS with a distance ratio d/D = 0.61, as shown in Fig. 8 (c) and (d). The vibration frequency of rippled SLGS decreases sharply from 0.4 THz to 0.05 THZ. Carbon atoms in SLGS are obviously restrained by CNT, and the inhibiting effect is closely related to the distance between CNT and SLGS, the length to diameter ratio of CNT, the effect length and direction of CNT.

In Fig. 9 (a), a phase diagram can be proposed to guide the design of nano resonator devices for potential applications. In Fig. 9 (b), we propose an idea of a graphene-based nano resonant device with tunable vibration frequency, which is modified by functional groups, defects, spontaneous wrinkles or CNT. The novel nano device can be anticipated to have a wide-range frequency shift as evident from Fig. 9 (a). Obviously, spontaneous wrinkles are most helpful to realize the vibration frequency maximization, with a relatively wide bandwidth ($\Delta f = 0.05$ THz). Another considerable measure of nano resonator is the normalized width of the resonance peak characterized by the quality factor $Q = f/\Delta f$ [8]. It is vital to promote the quality factor of nano resonator device as it increases the sensitivity of the resonator to external perturbation. To reduce the vibration frequency of the resonator, van der Waals interaction-driven rippled SLGS is the best choice, seen in Fig. 10. However, the extremely low quality factor makes it excluded in specific applications. Although the vibration frequency enhancing effect of SLGS with vacancy defects is not as significant as that of load-driven SLGS with surface wrinkles, its high quality factor increases the sensitivity and efficiency.

The current research systematically studies the vibration frequency response for functionalized SLGSs, graphene with defects, graphene under applied load and atomic interaction. Whereas their combinations may incur more fascinating physical properties, and develop the design space of nano resonator devices in the next generation. Before concluding, we hope the rippled graphene with multiple coupling factors will raise more attentions, and the further research will be performed in the near future.

4. Conclusions

In summary, this research has revealed the vibration frequency response of SLGSs with various rippled configurations through theoretical analysis. The resultant buildup of theoretical framework with regard to frequency shift would benefit the exploitation of nano devices. Several remarkable conclusions are as follows.

(1) Ripples have a significant influence on the surface configuration of SLGSs which is closely related to the variable vibration mass and strain energy, resulting in approximately 12.5%–150% frequency shift on SLGSs.
(2) The vibration frequency of SLGS is sensitive to the distribution manners of functional groups or defects. The continuously distributed ripples can efficiently increase the vibration frequency of SLGS, which is highly dependent on the strain energy.
(3) Vibration frequency reduction of SLGS with random ripples is mainly dominated by the variable mass. Functional groups (such as
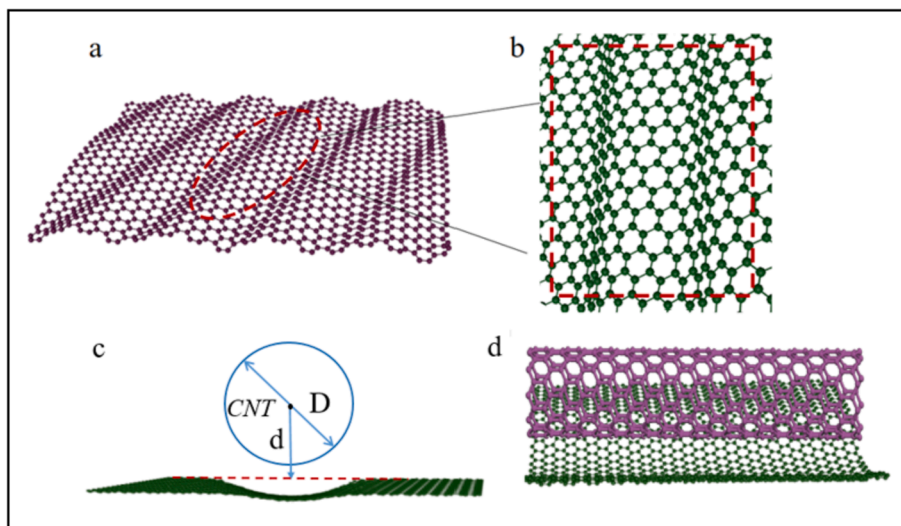

Fig. 8. Load-driven and van der Waals interaction-driven rippled SLGS: (a) Rippled SLGS with surface wrinkles. (b) Enlarged local wrinkle morphology. (c) Ripple on SLGS due to an Armchair CNT above the surface with a ratio d/D = 0.61. The diameter of CNT (D) is 3 nm. (d) Optimized model Armchair CNT of and SLGS. (A colour version of this figure can be viewed online.)
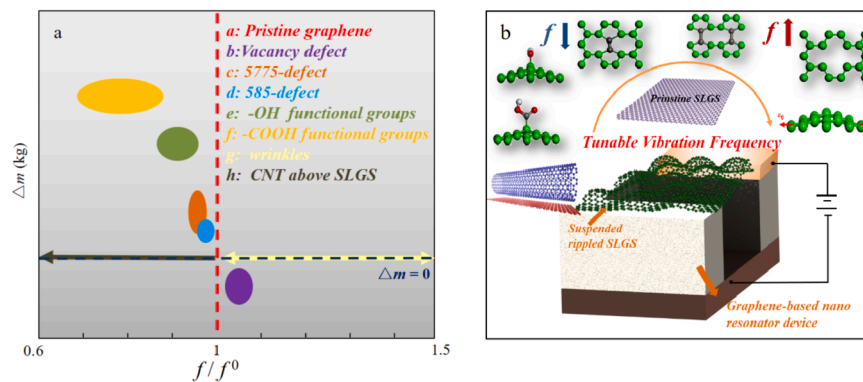
Fig. 9. (a) The phase diagram of different kinds of ripples-induced factors and vibration frequency shift. (b) The description of a graphene-based nano resonant device with tunable vibration frequency. (A colour version of this figure can be viewed online.)
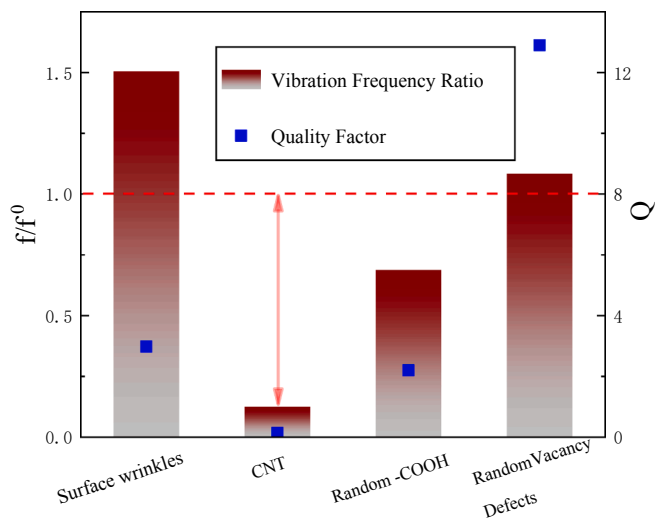

Fig. 10. Contrasts of the vibration frequency ratio and quality factor of different kinds of rippled SLGS. (A colour version of this figure can be viewed online.)

–COOH and –OH) and defects (such as 5775-defects and 585-defects) can reduce the frequency.
(4) Load-driven ripples can significantly enhance the vibration frequency, which corresponds to a wide bandwidth. The van der Waals interaction-driven ripples lead to an obvious reduction of vibration frequency with counterintuitive expectation of quality factor.
(5) The obtained results can provide a fundamental understanding of graphene vibration behavior and an insight for the next generation nano resonant devices design.

Conflicts of interest

The authors declared that we have no conflicts of interest to this work. We declare that we do not have any commercial or associative interest that represents a conflict of interest in connection with the work submitted.

Acknowledgements

References

[1] A.K. Geim, K.S. Novoselov, The rise of graphene, Nat. Mater. 6 (2007) 183–191.
[2] A.K. Geim, Graphene: status and prospects, Science 324 (2009) 1530–1534.
[3] M. Ge, C. Si, Mechanical and electronic properties of lateral graphene and hexagonal boron nitride heterostructures, Carbon 136 (2018) 286–291.
[4] G. Naumis, S. Barraza-Lopez, M. Oliva-Leyva, et al., Electronic and optical properties of strained graphene and other strained 2D materials: a review, Rep. Prog. Phys. 80 (2017).
[5] A. Sakhaee-Pour, M.T. Ahmadian, R. Naghdabadi, Vibrational analysis of single-layered graphene sheets, Nanotechnology 19 (2008).
[6] B. Arash, J.W. Jiang, T. Rabczuk, A review on nanomechanical resonators and their applications in sensors and molecular transportation, Appl. Phys. Rev. 2 (2015).
[7] R.W. Jiang, Z.B. Shen, G.J. Tang, Vibration analysis of a single-layered graphene sheet-based mass sensor using the Galerkin strip distributed transfer function method, Acta Mech. 227 (2016) 2899–2910.
[8] J.S. Bunch, A.M.V.D. Zande, S.S. Verbridge, et al., Electromechanical resonators from graphene sheets, Science 315 (2007) 490–493.
[9] S. Stankovich, D.A. Dikin, G.H.B. Dommett, et al., Graphene-based composite materials, Nature 442 (2006) 282–286.
[10] M.D. Stoller, S. Park, Y. Zhu, et al., Graphene-based ultracapacitors, Nano Lett. 8 (2008) 3498–3502.
[11] F. Schwierz, Graphene transistors, Nat. Nanotechnol. 5 (2010) 487–496.
[12] A. Fasolino, J.H. Los, M.I. Katsnelson, Intrinsic ripples in graphene, Nat. Mater. 6 (2007) 858–861.
[13] F. Scarpa, S. Adhikari, A.S. Phani, Effective elastic mechanical properties of single layer graphene sheets, Nanotechnology 20 (2009).
[14] B.N. Chandrashekar, A.S. Smitha, Y. Wu, et al., A universal stamping method of graphene transfer for conducting flexible and transparent polymers, Sci. Rep. 9 (2019).
[15] A. Reina, X. Jia, J. Ho, et al., Large area, few-layer graphene films on arbitrary substrates by chemical vapor deposition, Nano Lett. 9 (2009) 30–35.
[16] X. Li, W. Cai, J. An, et al., Large-area synthesis of high-quality and uniform graphene films on copper foils, Science 324 (2009) 1312–1314.
[17] K.S. Kim, Y. Zhao, H. Jang, et al., Large-scale pattern growth of graphene films for stretchable transparent electrodes, Nature 457 (2009) 706–710.
[18] J.C. Meyer, A.K. Geim, M.I. Katsnelson, et al., The structure of suspended graphene sheets, Nature 446 (2007) 60–63.
[19] Y.Z. He, H. Li, P.C. Si, et al., Dynamic ripples in single layer graphene, Appl. Phys. Lett. 98 (2011).
[20] K. Iyakutti, V.J. Surya, K. Emelda, et al., Simulation of ripples in single layer graphene sheets and study of their vibrational and elastic properties, Comput. Mater. Sci. 51 (2012) 96–102.
[21] B. Amorim, A. Cortijo, F.D. Juan, et al., Novel effects of strains in graphene and other two dimensional materials, Phys. Rep. 617 (2015) 1–54.
[22] E. Mahmoudinzhad, R. Ansari, Vibration analysis of circular and square single-layered graphene sheets: An accurate spring mass model, Physica E 47 (2013) 12–16.
[23] S. Jiang, S. Shi, X. Wang, Nanomechanics and vibration analysis of graphene sheets via a 2D plate model, J. Phys. D Appl. Phys. 47 (2014).
[24] T.J. Prasanna Kumar, S. Narendar, S. Gopalakrishnan, Thermal vibration analysis of monolayer graphene embedded in elastic medium based on nonlocal continuum mechanics, Compos. Struct 100 (2013) 332–342.
[25] C.G. Wang, L. Lan, Y.P. Liu, et al., Functional group-guided variable frequency characteristics of a graphene resonator, RSC Adv 3 (2013) 16095–16101.
[26] Norio Inui, Equilibrium shape of a suspended graphene sheet under electrostatic and van der Waals forces, J. Phys. D Appl. Phys. 51 (2018).
[27] J. Atalaya, A. Isacsson, J.M. Kinaret, Continuum elastic modeling of graphene resonators, Nano Lett. 8 (2008) 4196–4200.
[28] Y. Zhang, Z.X. Lei, L.W. Zhang, et al., Nonlocal continuum model for vibration of single-layered graphene sheets based on the element-free kp-Ritz method, Eng. Anal. Bound. Elem. 56 (2015) 90–97.
[29] S. Kitipornchai, X.Q. He, K.M. Liew, Continuum model for the vibration of

multilayered graphene sheets, Phys. Rev. B 72 (2005).

[30] R. Ansari, H. Rouhi, S. Sahmani, Free vibration analysis of single- and double-walled carbon nanotubes based on nonlocal elastic shell models, J. Vib. Control 20 (2014) 670–678.

[31] Y.W. Wong, S. Pellegrino, Wrinkled membranes Part II: analytical models, J. Mech. Mater. Struct. 1 (2006) 27–61.

[32] D. Garcia-Sanchez, A.M.V.D. Zande, A.S. Paulo, et al., Imaging mechanical vibrations in suspended graphene sheets, Nano Lett. 8 (2008) 1399–1403.

[33] B. Mortazavi, G. Cuniberti, T. Rabczuk, Mechanical properties and thermal conductivity of graphitic carbon nitride: A molecular dynamics study, Comp. Mater.

Sci. 99 (2015) 285–289.

[34] A.M.V.D. Zande, R.A. Barton, J.S. Alden, et al., Large-scale arrays of single-layer graphene resonators, Nano Lett. 10 (2010) 4869-487.

[35] C.G. Wang, L. Lan, Y.P. Liu, et al., Vibration characteristics of wrinkled single-layered graphene sheets, Int. J. Solids Struct. 50 (2013) 1812–1823.

[36] Y.P. Liu, C.G. Wang, L.M. Zhang, et al., An evaluation method for nanoscale wrinkle, Physica E 80 (2016) 191–194.

[37] Z.M. Xia, C.G. Wang, H.F. Tan, Elastic properties of graphene: a pseudo-beam model with modified internal bending moment and its application, Physica E (98) (2017) 45–52.